THE JOURNAL OF PHYSICAL CHEMISTRY B

ARTICLE

pubs.acs.org/JPCB

Measuring Local Equilibrium Flavor Distributions in SDS Solution Using Headspace Solid-Phase Microextraction

Nathan W. Lloyd,[†,‡] Eleni Kardaras,[‡,∥] Susan E. Ebeler,[§] and Stephanie R. Dungan*[,†,‡]

[†]Department of Chemical Engineering and Materials Science, [‡]Department of Food Science and Technology, and [§]Department of Viticulture and Enology, University of California, Davis, One Shields Avenue, Davis, California 95616, United States

ABSTRACT: Solid-phase microextraction (SPME) sampling of the headspace above an aqueous micellar solution of sodium dodecyl sulfate (SDS) was shown to be effective for quantifying the equilibrium partitioning of limonene solute between water and SDS micellar aggregates. Concentrations in the headspace were determined from the amount absorbed by the SPME fiber during 1 min extractions, with the quantity on the fiber determined using gas chromatography/mass spectrometry (GC/MS). Headspace concentrations as a function of surfactant concentration were fit to a mass balance to yield the partition coefficient and critical micelle concentration. When the total limonene in the system was low enough that it could be completely dissolved by water in the absence of micelles, a constant value for the partition coefficient of 1700 M^{-1} was obtained, independent of the limonene concentration. However, at higher total limonene concentrations, the partition coefficient became a function of the amount of limonene in the micelles, as confirmed by separate experiments in which either limonene or SDS concentration was varied. The observed increase in partition coefficient with increasing limonene likely signals a shift from micelles to swollen micelles and ultimately to microemulsion droplets. The effect of SDS concentration on the aqueous solubility limit of limonene could also be observed in HS-SPME experiments where either SDS or limonene was varied.

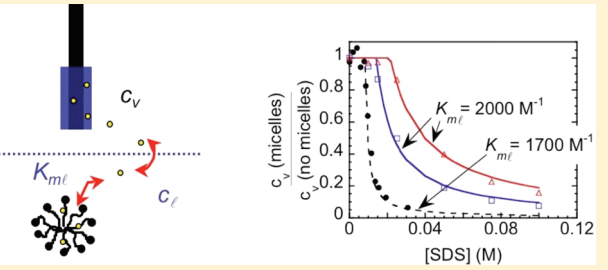

INTRODUCTION

Amphiphilic molecules will often self-assemble within water to form aggregates known as micelles. Within these micelles, a hydrophobic nanodomain is created by the nonpolar tails of the amphiphiles. As a result, micelles can usefully host, or "solubilize", poorly water-soluble, hydrophobic compounds within an aqueous solution, and this has led to applications for these solutions in areas such as drug delivery,[1,2] environmental remediation,[3,4] consumer products and food formulations,[5−7] and in analytical and reactor technologies.[8−10] Micellar solubilization also plays an important role in the absorption of hydrophobic food compounds in the gastrointestinal tract.[11,12] In understanding and capitalizing on solubilization properties of micelles in these different arenas, information is needed on the local partitioning of solute compounds between the micelles and the surrounding aqueous continuum. Such information is necessary, for example, to determine the effectiveness of micelles in enhancing water solubility of the compound, to assess potential for chemical or biological transformation of compounds, and to predict rates of solute release. In this Article, we describe application of headspace solid-phase microextraction (HS-SPME) as a simple, noninvasive, and quantitatively accurate method for determining the local distribution of hydrophobic solutes within an aqueous micellar solution. The approach we use is conceptually similar to that developed previously for measuring binding or partitioning of solutes to sorptive materials, such as soils, membranes, and proteins.[13−16]

Various methods have been proposed for measuring partition coefficients for solutes distributing between micelles and the continuous phase.[17−25] Often such methods are specific for certain types or classes of solutes, such as fluorescent solutes whose local environment can be probed using quenching methods, dyes with ionization equilibria that can be detected spectrophotometrically, or polar compounds that have non-negligible contributions to overall solution properties from both solubilized and free solute. Recently, static headspace chromatographic approaches have received increased attention as a convenient and general way to measure solute partitioning within micellar solutions.[7,26−30] Originally developed for investigating alkanol solutes with 4−6 carbons,[31] such approaches can also be applied to highly nonpolar, volatile solutes. The micellar solution with known total concentration of surfactant and solute is allowed to equilibrate with a vapor (headspace) phase in a closed vial. Analysis of the headspace by gas chromatography provides information on the concentration of solute dissolved directly in the aqueous continuum, based on known vapor/water partition coefficients. From this information, the micelle/aqueous solution partitioning is determined.

In this Article, we have adapted the above approach to take advantage of SPME techniques. SPME fibers are coated with a

Received: July 21, 2011
Revised: October 12, 2011
Published: October 17, 2011

Table 1. GC/MS Parameters for Experiments Measuring Limonene Partitioning at Low and High Total Limonene Concentration, Relative to the Solubility of Limonene in Water Alone

	$n_{tot}/(V_{\ell}c_{\ell}^{sat}) < 1$	$n_{tot}/(V_{\ell}c_{\ell}^{sat}) > 1$
inlet mode	splitless	40:1 or 200:1 split ratios[a]
column flow rate (mL/min)	0.9 mL/min	1.0 mL/min
GC oven program	50 °C, +5 °C/min to 100 °C, +40 °C/min to 250 °C	40 °C, +5 °C/min to 75 °C, +40 °C/min to 240 °C
GC/MS interface temperature	260 °C	240 °C
MS parameters	scan mode; m/z = 15−150 at 5.25/s	selected ion monitoring mode; m/z = 68[b]

[a] The "Gas Saver" feature was used to reduce the split flow to 20 mL/min starting 3 min after insertion of the SPME fiber into the inlet. [b] Most abundant ion fragment.

thin absorptive film, which allows one to quantitatively probe solute concentrations in the headspace above a micellar solution. SPME offers several advantages in this context over static headspace sampling. Most significantly, the fibers selectively absorb and concentrate solute from the vapor phase, and thus provide increased sensitivity to those headspace concentrations, relative to static sampling. This allows the method to be extended to solutes with lower volatilities, or those with low concentrations within the aqueous continuum. Through selection of various absorptive coatings on the SPME fiber, solutes of a range of polarities can be sampled, and the potential for selective detection of solutes within multisolute systems also exists. The lower sample volumes injected into the gas chromatography column, as compared to conventional headspace GC methods, reduce wear on the column and help to make the former an inexpensive, convenient, and reproducible approach for these applications. With these advantages, the possibility of using HS-SPME for measuring partitioning of hydrophobic solutes is of particular interest. As compared to more polar molecules, the distribution of hydrophobic compounds into micelles has received less attention:[32] their low solubility in water requires a method with high sensitivity, and any loss of solute from the closed system can introduce significant errors. The sections below describe our adaptations of HS-SPME for sampling hydrophobic compounds in a closed system containing a micelle solution, and our successful application of this approach for studying the flavor compound limonene. Limonene is a nonpolar and hydrophobic flavoring agent that is widely used in food and beverages, and has a solubility c_{ℓ}^{sat} in water alone of 13.8 mg/L, or 1.01×10^{-4} M.[33]

Our method is complementary to one recently developed by Pino and co-workers,[34] in which SPME fibers are used to sample solute from the aqueous solution itself. This mode of fiber microextraction is known as "direct immersion", or DI-SPME. DI-SPME has been used to determine micelle/water partition coefficients for polyaromatic hydrocarbons[34,35] and phenolic compounds.[36] HS-SPME and DI-SPME each have their advantages. DI-SPME would be most appropriate for solutes with very limited volatility. HS-SPME, on the other hand, would be more sensitive to volatile components with very low water solubilities and has the benefit of distinguishing such solutes from nonvolatile components of the aqueous solution that may absorb to the SPME fiber during direct immersion. Ideally, a micellar solution could be probed using both HS-SPME and DI-SPME, to obtain more complete information on the distribution of components within the solution.

In this study, HS-SPME measurements were used to determine equilibrium distributions in vials containing various sodium dodecyl sulfate concentrations and low total amounts of solute. The total moles of limonene n_{tot} for these experiments, divided by the liquid volume V_{ℓ}, was less than the solubility limit of limonene in water alone. In this regime, the HS-SPME method determined a constant partition coefficient $K_{m/}$ that characterizes the solute distribution between micelle and water. Studies were also performed at higher limonene concentrations, $n_{tot}/(V_{\ell}c_{\ell}^{sat}) > 1$, where the behavior as a function of [SDS] was more complex. Finally, HS-SPME was used to obtain the entire solubilization isotherm for limonene partitioning as a function of solute concentration at a constant micelle concentration. Such solubilization isotherms, which have previously received attention from only a few investigators,[26,28,31,37−40] reveal effects on the partitioning behavior of increasing amounts of solute within the micelle.

EXPERIMENTAL METHODS

Limonene (MW 136.24 g/mol) was purchased from Sigma-Aldrich (St. Louis, MO) with 98% purity. Sodium dodecyl sulfate (98% pure) was supplied by USB Corp. (Cleveland, OH). Deionized water used in sample preparations was obtained from a Milli-Q water purification system installed in the laboratory (Millipore, Bedford, MA).

The identification and quantification of limonene was achieved using headspace solid-phase microextraction and gas chromatography/mass spectrometry. GC/MS analysis was performed on two different instruments: a Hewlett-Packard GC series 6890 with a 5973 MSD (GC/MS 1) and an Agilent Technologies 6890N GC with a 5975 MSD (GC/MS 2). A DB-wax column (30 m × 0.25 mm i.d. × 0.25 μm film thickness) was used in both instruments (Agilent, Santa Clara, CA). For all experiments, the SPME fiber was exposed to the headspace for 1 min, followed by desorption in the GC inlet for 10 min. 85 μm polyacrylate (PA) fibers (Supelco, Bellefonte, PA) were conditioned in a GC inlet set at 300 °C for 2 h, as specified by the manufacturer. Table 1 lists the parameters used in our GC/MS analysis, which depended on the ratio of total moles of limonene (n_{tot}) added to the vial, relative to the moles of limonene that would dissolve at its solubility limit in the added water volume V_{ℓ}. This latter quantity is given by $V_{\ell}c_{\ell}^{sat}$. At the inlet to the GC, a splitless mode was used only for experiments with low total limonene concentrations, because the split mode was needed to accommodate higher amounts extracted from systems with higher total limonene. The oven program consisted of an initial temperature, a first constant ramping of temperature up to an intermediate value, and a second ramp to a final temperature. Oven conditions were optimized to provide sufficient throughput without limiting the ability to quantitatively

analyze the limonene peak. Dropping the customary initial temperature hold had no effect on peak shape. Helium (99.999%, Airgas, Woodland, CA) was used as the carrier gas at a constant flow rate. Agilent/HP Chemstation software was used on both instruments.

A portion of the experiments were performed with low limonene concentrations ($n_{tot}/(V_{\ell}c_{\ell}^{sat}) < 1$), varying SDS concentration at constant V_{ℓ} and n_{tot}. To prepare samples for such experiments, headspace vials were partially filled with an aqueous SDS solution, created by diluting a 3 wt % SDS stock solution with water. The concentration of SDS ranged from 0 to 0.1 M, corresponding to data points below and above the critical micelle concentration (*cmc*, 8 mM[41]). To achieve low solute concentrations, the limonene was first dissolved in dimethyl sulfoxide (DMSO, 99.9%) from Fisher Scientific (Fair Lawn, NJ) to form stock solutions with concentrations of $(6.19-61.9) \times 10^{-4}$ M. Portions of these stock solutions were added to the aqueous solutions in the headspace vials to achieve the desired solute concentration. Several different concentrations of limonene in DMSO were utilized to determine the effect of the analyte concentration on partition coefficients. The lower limit of limonene concentration was chosen so that it provided peak areas at least 5 times higher than the noise signal on the GC/MS at the highest surfactant concentration. DMSO concentrations in the final solutions were always less than 0.02 wt %,[42] too low to affect limonene partitioning in the system.[43,44]

Sample vials were also prepared with high limonene concentrations such that, in the absence of the surfactant, the amount of limonene per aqueous volume exceeded the solubility limit in water ($n_{tot}/(V_{\ell}c_{\ell}^{sat}) > 1$). For these solutions, 1.5 or 3 μL of neat limonene was added directly to 12 mL vials containing 5 mL of aqueous solution of various SDS concentrations. A similar procedure was used to prepare 12 mL sample vials with various total amounts of limonene, which were added directly to 5 mL of 0.015 M SDS aqueous solution. These systems were all analyzed on GC/MS 2.

The vials were capped using a specially created,[43] quadruple barrier consisting of a PTFE gasket (19.1 mm o.d. × 14.0 mm i.d. × 0.13 mm, Metro Gasket, Kansas City, MO), a disk of aluminum foil (Reynolds, Richmond, VA), a PTFE/silicone septum of 3 mm thickness (SUN SRi, Duluth, GA), and a bimetal (Sn/Al) crimp cap (SUN SRi, Duluth, GA). Vials were incubated in a shaker bath at room temperature (25 °C). For experiments in which SDS was varied at low limonene concentrations, an incubation time of 20 min was used. For experiments in which SDS was varied at high limonene concentrations, an incubation time of 5.5 h was used. For experiments in which the limonene concentration was varied for constant [SDS], the vials were incubated for 1 h.

The samples were then randomized and placed in the auto sampler trays for data collection. For SPME analysis with GC/MS 1, a Varian 8200CX 12 vial auto sampler was used (Walnut Creek, CA). For samples run on GC/MS 2, a 32 vial Gerstel MPS2 auto sampler (Linthicum, MD) was used, allowing more samples to be analyzed in the same run. It should be noted that because a run time of 18.75 min was necessary for each sample and all samples were prepared at the same time, the last sample would have been sampled several hours after the first. It was found that allowing some samples more time in the auto sampler tray before sampling did not affect the results, indicating that the samples had already reached equilibrium after the incubation period.

ANALYSIS OF PARTITIONING

The mole balance on solute in a system containing n_{tot} total moles can be written as

$$n_{tot} = \frac{x_m}{1-x_m} n_{surf} + c_v V_v + c_{\ell} V_{\ell} + c_f V_f \approx \frac{x_m}{1-x_m} n_{surf} + c_v V_v + c_{\ell} V_{\ell} \quad (1)$$

Here, c_v, c_{ℓ}, and c_f are the concentrations in the vapor, liquid, and fiber film phases, respectively, and V_v, V_{ℓ}, and V_f are the corresponding vapor, liquid, and fiber film volumes. The amount of solute in the micelles is represented by the first term, which depends on the mole fraction x_m of solute in the micelle and on the n_{surf} moles of surfactant in micelles.

The amount of solute in the fiber is often neglected in this mole balance.[34] Some SPME applications employ a long extraction time that allows the solute to equilibrate completely between the different environments represented in eq 1. For such long extraction times, neglect of the term $c_f V_f$ requires that the system satisfy the constraint, $K_{f\ell} \ll V_{\ell}/V_f$ for DI-SPME, or $K_{fv} \ll V_v/V_f$ for HS-SPME. Here, $K_{f\ell}$ and K_{fv} are the liquid−film or vapor−film partition coefficients, defined as the equilibrium film concentration divided by that in the adjacent continuous phase. Given the small volume of the fiber film relative to the sample vial, these conditions are often satisfied even for many hydrophobic solutes.

However, in our work, the above constraints are unnecessarily restrictive. Our experiments employ a short extraction time of 1 min, which is 2 orders of magnitude shorter than the time required for the fiber to reach equilibrium.[34] Consequently, the amount of solute on the fiber will be proportionately lower, and the neglect of the $c_f V_f$ term is even more easily justified. Under these conditions, the amount of solute extracted into the fiber is negligible relative to the remainder of the system and is assumed to be proportional to the concentration in the phase surrounding the fiber, that is, $c_f \propto c_v$ for headspace SPME.

The equilibrium distribution of solute between the micelle interior and the aqueous continuum is typically represented through a micelle−liquid partition coefficient $K_{m\ell}$:

$$K_{m\ell} = \frac{x_m}{c_{\ell}} \quad (2)$$

The presumption that $K_{m\ell}$ is a constant at constant temperature and pressure, that is, is independent of concentration, relies on low concentrations of solute in both the aqueous and the micellar pseudophases, a constraint that will be evaluated in our experiments. Under these conditions, we may also assume that the concentration of solute inside the micelle is low enough that $1 - x_m \approx 1$.

Definition 2, together with the gas−liquid partition coefficient, $K_{v\ell} = c_v/c_{\ell}$, can be used to replace c_{ℓ} in eq 1, yielding

$$n_{tot} = \frac{c_v}{K_{v\ell}} K_{m\ell}(c_{surf} - cmc)V_{\ell} + c_v V_v + \frac{c_v}{K_{v\ell}} V_{\ell} \quad (3)$$

In the first term on the right, the amount of surfactant in micelles is determined from the difference between the total surfactant

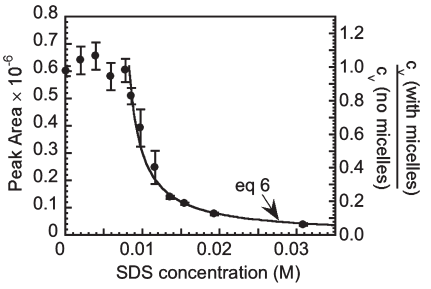

Figure 1. Measured peak area (left axis) of limonene extracted from the vapor phase above an SDS solution; error bars represent 95% confidence intervals. Total limonene corresponded to $n_{tot}/(c_{/}^{sat}V_{/}) = 0.0068$. Values on the right axis are normalized by the average peak area below the *cmc*. Solid line is the fit of eq 6 to the latter data, with $K_{v/} = 1.6$, $V_{/}/V_v = 1.3$.

concentration c_{surf} and the critical micelle concentration. Equation 3 rearranges to

$$n_{tot} = \frac{A}{k}\left[V_{/}\frac{K_{m/}(c_{surf} - cmc) + 1}{K_{v/}} + V_v\right]$$

where A is the peak area in the GC obtained from the fiber extraction, and k is a proportionality constant. In this result, we have used the direct relation between gas-phase concentration and the amount of solute on the fiber, which is in turn proportional to A. As a result, the peak area can be related to experimental and physical parameters as

$$A = \frac{n_{tot}kK_{v/}}{(K_{m/}(c_{surf} - cmc) + 1)V_{/} + V_vK_{v/}} \quad (4)$$

In eq 4, n_{tot}, c_{surf}, $V_{/}$, and V_v are controlled experimentally. Thus, determination of $K_{m/}$ requires only that we have information about the *cmc* and $K_{v/}$. In the limiting case of solute partitioning in water/vapor systems, eq 4 becomes

$$A = \frac{n_{tot}kK_{v/}}{V_{/} + V_vK_{v/}} \quad (5)$$

Therefore, experiments measuring A versus n_{tot} for various ratios of $V_{/}$ to V_v in the absence of surfactant yield the required values of k and $K_{v/}$. We have performed such experiments for several hydrophobic compounds.[43] The value for limonene of $K_{v/} = 1.6$ used in this work was taken from Helburn and co-workers.[45]

RESULTS AND DISCUSSION

Headspace Concentration Variation with Surfactant Concentration. $K_{m/}$ can be determined from two types of experiments. A can be measured as a function of n_{tot}, holding the surfactant concentration constant, or one can measure A versus c_{surf} at constant n_{tot}. In Figure 1, results from the latter type of experiment are presented. In these experiments, the total amount of limonene was held constant at 6.19 nmol, and the 16 mL vials were filled with 9 mL of liquid. This corresponds to a value of $n_{tot}/(c_{/}^{sat}V_{/}) = 0.0068$, where $c_{/}^{sat} = 1.01 \times 10^{-4}$ M is the saturation concentration of limonene in water.[33] It is apparent from the results in Figure 1 that for low surfactant concentrations $c_{surf} < cmc$, the peak area was independent of SDS concentration within experimental error. This observation indicates that the presence of the SDS monomer had no measurable effect on limonene vapor−liquid partitioning. As SDS concentration was increased above the *cmc*, a steep decrease in the limonene volatility was observed, as limonene increasingly solubilized within the micelles.

Because the addition of SDS below the *cmc* does not significantly modify limonene volatility, the peak area should be well described at these concentrations by eq 5, with $K_{v/}$ obtained from independent water/vapor experiments. A value for the product $n_{tot}k$, and in turn, k, can thereby be determined from the average of the peak areas in this concentration range. A still simpler approach is to divide the data shown in Figure 1 by the average peak area below the *cmc*, yielding the ratio of vapor phase concentration of limonene above a micellar solution to that above water alone. This ratio is plotted on the right axis of Figure 1. These concentration ratios are represented theoretically by the ratio of eqs 4 and 5:

$$\frac{c_v(\text{micelles})}{c_v(\text{no micelles})} = \frac{1 + K_{v/}V_v/V_{/}}{K_{m/}(c_{surf} - cmc) + K_{v/}V_v/V_{/} + 1} \quad (6)$$

This approach essentially treats the limonene samples without micelles as a reference standard, thus eliminating some day-to-day variation in the fiber or instrument (and thus in k) as a source of error.

Several experiments such as that shown in Figure 1 were conducted to obtain vapor phase concentration ratios as a function of aqueous SDS concentration. The data set from each of these experiments was fit to eq 6, using a Levenberg−Marquardt nonlinear least-squares numerical optimization algorithm. For example, the data in Figure 1 are shown with the curve corresponding to eq 6, fitting $K_{m/}$. Given that the critical micelle concentration is a value readily available in the literature, one option for analyzing each experiment was to fix the *cmc* and fit only $K_{m/}$ in eq 6. However, comparison of five sample sets (each containing a range of SDS concentrations), obtained on five separate days, indicated that results of fits for $K_{m/}$ to each data set exhibited less variability between different sample sets, that is, were more reproducible, when the *cmc* was used as a fit parameter. This comparison is given in Table 2. Although the average of the *cmc* values obtained from the fits agreed with the literature value within experimental error, the critical micelle concentration obtained from the fits was slightly higher than the literature value, and the associated $K_{m/}$ was also higher than for the case where the *cmc* was fixed. A higher *cmc* value would indicate a smaller concentration of micelles associated with the measured reduction in limonene vapor concentration, and this would thus imply a higher value for the partition coefficient.

The probable cause for the improvement in the consistency of the $K_{m/}$ fit results is a variation in the actual, physical *cmc* between experiments due to temperature variations. The experimental temperature varied from 25 to 29 °C, and the *cmc* has been found to vary roughly as 9×10^{-5} M/°C with temperature (Shah et al., 2001), yielding a variation in concentration similar in extent to what was observed experimentally (Table 2). Perhaps most significantly, the quality of our results demonstrates that HS-SPME is a noninvasive, convenient, and sensitive method for measuring the *cmc*.

As an alternative to using a nonlinear fit of eq 6 to the data in Figure 1, data could have been transformed to a plot of $1/A$

Table 2. Compared Average Values $\bar{K}_{m/} = (\sum_{i=1}^{5} K_{m/,i})/5$ and $\overline{cmc} = (\sum_{i=1}^{5} cmc_i)/5$, Obtained from Two Procedures for Fitting Eq 6 to Five Data Sets[a]

analysis	$\bar{K}_{m/} \pm \bar{\Delta}_K$[b] ($M^{-1}$)	standard deviation in $\bar{K}_{m/}$ (M^{-1})	$\overline{cmc} \pm \bar{\Delta}_{cmc}$[b] ($10^{-3}$ M)	standard deviation in $\overline{cmc}$ (10^{-3} M)
fix *cmc*	1600 ± 141	329	8.10 (fixed)	
fit *cmc*	1840 ± 68.4	160	8.30 ± 0.063	0.25

[a] Procedures consist of fitting $K_{m/}$ and either fitting or fixing the *cmc*, yielding $K_{m/,i} \pm \Delta_{K,i}$ and $cmc_i \pm \Delta_{cmc,i}$, or $K_{m/,i} \pm \Delta_{K,i}$ alone. $\Delta_{K,i}$ and $\Delta_{cmc,i}$ are the 95% confidence limits within each data set. [b] 95% confidence limits obtained as $\bar{\Delta}_K = ([\sum_{i=1}^{5} \Delta_{K,i}^2]^{1/2})/5$ or $\bar{\Delta}_{cmc} = ([\sum_{i=1}^{5} \Delta_{cmc,i}^2]^{1/2})/5$.

versus c_{surf}, with the expected linear relationship between these values yielding $K_{m/}$ through eq 4. However, this option was considered less accurate, because, in transforming the experimental data, experimental errors would be transformed in a nonlinear way. This is undesirable because the standard deviations of the peak areas for any given set of experimental conditions are expected to be normally distributed, as least-squares analyses typically assume, but the transformation would skew such distributions.

Distribution of Solute at Low Solute Concentrations. Measurements of *A* versus c_{surf} were carried out at different total solute concentrations within the closed vial system, keeping the total amount of limonene per unit volume of liquid well below the aqueous solubility $c_{/}^{sat}$ for limonene. The ratio of volumes between vapor and liquid phase was also varied. These studies enabled us to explore the influence of experimental errors, such as small amounts of leakage of solute from the vial, or inaccuracies in initial solute loading, on our results. More significantly, these studies were used to evaluate the assumption in our theory in which a constant partition coefficient is used to describe the partitioning of solute between micelle and aqueous pseudophase. At higher total concentrations of solute, this assumption may break down.

Total limonene concentrations were varied between 1.5×10^{-7} and 4×10^{-6} mol per liter of total volume within the vial. Phase ratios of liquid to vapor volume were 0.4 or 1.3. Plots of c_v(micelles)/c_v(no micelles) versus surfactant concentration were fit with eq 6; the correlation coefficient for these fits was greater than 0.970 in all cases. No significant difference was seen, within a 95% confidence interval, between values of $K_{m/}$ or the *cmc* obtained at these different concentrations and phase ratios. In the absence of surfactant (or below the *cmc*) and based on the known value for $K_{v/}$, these total concentrations represent aqueous concentrations that are 0.1−3% of the saturation concentration of limonene in water. Therefore, given that these samples were very far from approaching the solubility limit of the aqueous phase, it is not surprising that the assumption of a constant $K_{m/}$ worked very well in representing the data.

As surfactant concentration increases above the *cmc*, the limonene concentration in the aqueous continuum should decrease as the solute partitions more extensively into the micelles. On the basis of our results, at 40 mM surfactant, the limonene in water was reduced to a value that was 3% of that in the absence of micelles. However, despite the extensive removal of solute from water by the micelles, calculations from eqs 2 and 3 of the mole fraction x_m of solute in the micelles indicated that this fraction was always less than $\sim 5 \times 10^{-3}$. Thus, the assumption that the mole fraction of solute within the micelles is very small is well-justified. The mole fraction of limonene in the micelles is actually largest for surfactant concentrations closest to the *cmc*, where the aqueous concentration of limonene is largest and the moles of surfactant in the micelles is smallest. x_m decreases rapidly as [SDS] increases above the *cmc*.

Table 3. $K_{m/}$ Values for Limonene in Anionic Dodecyl Surfactant Solutions

reference	$K_{m/}$ (M^{-1})	micelle solution
Micke et al.[18]	3240	SDS in 20 mM tetraborate solution
Helburn et al.[45]	2086	sodium dodecylbenzene sulfonate (NaDBS) in water
This work	1700	SDS in water

Given that $K_{m/}$ and *cmc* were independent of the total limonene concentration at these low levels of [limonene], and independent of the ratio of liquid to vapor in the system, we can average all of the values obtained by analyzing all 47 sample sets using eq 6, with each set containing data taken as a function of SDS concentration. The results are $K_{m/} = 1700 \pm 73$ M^{-1} and $cmc = (8.27 \pm 0.20) \times 10^{-3}$ M (Table 3, 95% confidence level). The *cmc* result closely matches literature values of $(8.1-8.2) \times 10^{-3}$ M.[41,46]

There are no previous measurements of limonene partitioning into SDS micelles in water. In Table 3, we compare our results to measurements made in other, related micellar solutions. Micke et al.[18] used micellar electrokinetic chromatography to determine $K_{m/}$ values for limonene in SDS solutions that also contained 0.04 M tetraborate. Their value for the micelle/water partition coefficient is approximately twice as large as our result for SDS micelles in water alone. The presence of the tetraborate salt in the Micke et al.[18] (2003) study would be expected to increase the micellar aggregation number for SDS from 50 to approximately 80.[32] In addition, salting out effects from the tetraborate could increase the hydrophobicity of the limonene. Both of these effects would be likely to increase the solute partition coefficient. Micke et al.[18] also determined an experimental *cmc* value of 0.0058 ± 0.002 M for their system, lower than the *cmc* for SDS in water, a further indication of the influence of the added salt on the micellar properties.

We also analyzed recent results by Helburn et al.,[45] who examined the distribution of limonene into micelles containing sodium dodecylbenzenesulfonate (SDBS), an anionic surfactant with a structure somewhat similar to SDS. The authors used static sampling of the headspace to measure the concentration ratio of solute between the headspace (c_v) and the solution phase (c_{soln}) that contained surfactant. According to eqs 1 and 2, this concentration ratio can be represented by the equation:

$$\frac{c_v}{c_{soln}} = \frac{K_{v/}}{K_{m/}(c_{surf} - cmc) + 1} \quad (7)$$

We analyzed the four data points provided in this investigation with concentrations higher than the putative *cmc*, using eq 7 and fitting both $K_{m/}$ and the *cmc* (Figure 2). Values of $K_{m/} = 2086$ M^{-1} and *cmc* = 0.0045 M were obtained. The value for $K_{m/}$ is similar to, but somewhat higher than, our result for limonene in SDS. Stronger partitioning of limonene into the SDBS micelles is likely to result from the larger size of these structures as compared to SDS micelles and is promoted by the additional nonpolar benzene ring in the former surfactant.

On the other hand, the *cmc* value obtained from the data of Helburn et al.[45] is quite high as compared to the literature values for SDBS they report (0.00112−0.0015 M). However, fixing the *cmc* to a lower value made it impossible to fit the data with a single value for $K_{m\ell}$. Because the total limonene concentration in the sample vials was not explicitly stated in this work, we speculate that the total limonene was above that needed to saturate the water and vapor in the vial, and hence the concentration at which the discontinuity is observed may reflect not the *cmc*, but instead the point at which the system becomes saturated with limonene (cf., eq 9), as discussed in the section below.

Distribution of Solute at High Solute Concentrations. The partitioning behavior of limonene at concentrations well below its aqueous solubility limits was compared to results in mixtures with much higher limonene concentrations. The vapor phase concentration above surfactant solutions of various concentrations was determined for systems containing 7.71×10^{-4} or 1.54×10^{-3} mol of limonene per L of total volume in the vial. Normalizing the solute amount by the volume of liquid (5 mL) in the vial instead of the total (12 mL) volume yields 1.85×10^{-3} and 3.70×10^{-3} M for the two concentrations. These values are well above the solubility limit c_{ℓ}^{sat} for limonene in water alone (no surfactant): $n_{tot}/(c_{\ell}^{sat}V_{\ell}) = 18$ or 37 for the two values of n_{tot}.

Results for c_v, normalized by the average headspace concentration measured above water in the absence of surfactant, are presented in Figure 3. At high total amounts of limonene, the latter corresponds to the vapor phase concentration in equilibrium with either pure limonene or a saturated aqueous solution of limonene. Results from these experiments are compared to data presented in Figure 1 for systems with low limonene concentration. As in the previous experiment, c_v(micelles)/c_v(no micelles) ≈ 1 for low concentrations of SDS, and then decreased with increasing surfactant concentration above a certain value of [SDS]. As compared to the data at low [limonene], however, the drop in vapor phase concentration was less steep, and it occurred at SDS concentrations higher than the *cmc*. The SDS concentration where the decrease started also increased with increased total limonene in the system.

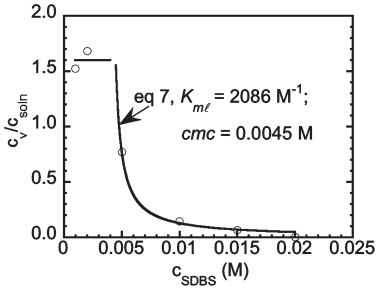

Figure 2. Static headspace data from Helburn et al.[45] for limonene in SDBS micelles. Curve is fit of eq 7 to find $K_{m\ell}$ and *cmc*.

To analyze these results, eqs 1−3 can be modified to accommodate the possibility of an excess, pure limonene phase in the vial. This excess phase would form when the micelle concentration is insufficient to completely solubilize limonene within the aqueous solution, so that

$$n_o = n_{tot} - c_{\ell}^{sat}V_{\ell}\left[\frac{K_{m\ell}}{1 - K_{m\ell}c_{\ell}^{sat}}(c_{surf} - cmc) + K_{v\ell}V_v/V_{\ell} + 1\right] \quad (8)$$

Here, n_o is the number of moles of limonene in the excess phase. When the total limonene is well in excess of the amount taken up by the aqueous surfactant solution, the amount dissolved in the water itself will be at its maximum, and therefore c_{ℓ} is set to c_{ℓ}^{sat} in eq 8. In eq 8, we have also accounted for the possibility that at higher values of n_{tot}, we can no longer assume that $1 - x_{mic} \approx 1$ in the first term of eq 1.

Setting $n_o = 0$ in eq 8 enables one to predict the minimum surfactant concentration $c_{surf,o}$ required to completely solubilize n_{tot} total moles of limonene in the system:

$$c_{surf,o} = cmc + \frac{1 - K_{m\ell}c_{\ell}^{sat}}{K_{m\ell}}\left[\frac{n_{tot}}{c_{\ell}^{sat}V_{\ell}} - K_{v\ell}\frac{V_v}{V_{\ell}} - 1\right] \quad (9)$$

This result applies only for $n_{tot}/(c_{\ell}^{sat}V_{\ell}) > (1 + K_{v\ell}V_v/V_{\ell})$, because for lower values of n_{tot}, $c_{\ell} < c_{\ell}^{sat}$ and the water alone can take up the necessary solute, even in the absence of micelles. For $n_{tot}/(c_{\ell}^{sat}V_{\ell}) > (1+K_{v\ell}V_v/V_{\ell})$, on the other hand, eq 9 yields the surfactant concentration above which the excess limonene phase disappears and the vapor phase concentration of limonene begins to decrease with increasing SDS concentration. When $c_{surf} < c_{surf,o}$, the vapor phase concentration will remain constant at $c_v = c_v^{sat}$. These trends are clearly exhibited by the data sets with $n_{tot}/(c_{\ell}^{sat}V_{\ell}) = 18$ and 37 in Figure 3. The critical concentration $c_{surf,o}$ in eq 9 increases with increased $n_{tot}/(c_{\ell}^{sat}V_{\ell})$, a prediction also borne out by the data.

When the surfactant concentration exceeds $c_{surf,o}$, the peak area obtained from sampling the vapor phase is still given by eq 4. This peak area is now normalized by $A = kc_v^{sat}$, the expected result

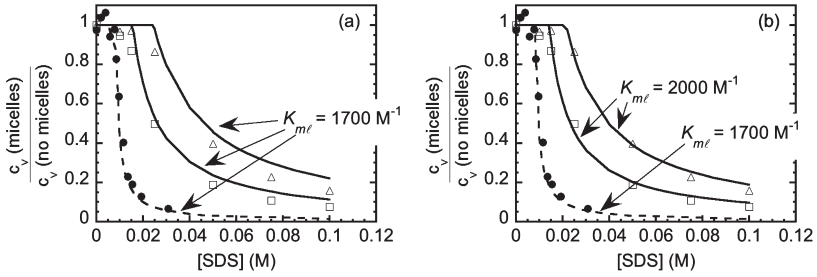

Figure 3. Normalized vapor phase concentration of limonene above an aqueous SDS solution, at total limonene levels well below ($n_{tot}/(c_{\ell}^{sat}V_{\ell}) = 0.068$, ●) and well above the aqueous solubility of limonene in water ($n_{tot}/(c_{\ell}^{sat}V_{\ell}) = 18$, □; or $n_{tot}/(c_{\ell}^{sat}V_{\ell}) = 37$, △). Curves are fits of eq 6 (− − −) or predictions of eq 11 (−) with (a) $K_{m\ell} = 1700$ M^{-1} for all data, or (b) $K_{m\ell} = 1700$ M^{-1} for $n_{tot}/(c_{\ell}^{sat}V_{\ell}) < 1$, $K_{m\ell} = 2000$ M^{-1} for $n_{tot}/(c_{\ell}^{sat}V_{\ell}) > 1$.

in the absence of micelles. Thus, the data in Figure 3 for higher [limonene] should be quantitatively predicted by

$$\frac{c_v\ (\text{micelles})}{c_v\ (\text{no micelles})} = \frac{c_v}{c_v^{sat}} = \frac{n_{tot}}{c_\ell^{sat} V_\ell} \frac{1}{\frac{K_{m\ell}}{1 - K_{m\ell} c_\ell^{sat} c_v / c_v^{sat}} (c_{surf} - cmc) + K_{v\ell} V_v / V_\ell + 1} \quad (10)$$

where we have used the relation $K_{v\ell} = c_v^{sat}/c_\ell^{sat}$. As discussed above, eq 10 reflects the more accurate representation of moles inside the micelles for the case where $1 - x_{mic} \neq 1$. As a result, this equation is no longer an explicit result for c_v/c_v^{sat}. To obtain our prediction for the measured, normalized vapor phase concentration, it is necessary to solve the quadratic equation that results from rearrangement of eq 10, that is

$$\frac{c_v}{c_v^{sat}} = \frac{B - \sqrt{B^2 - 4AC}}{2A} \quad (11)$$

where

$$A \equiv K_{m\ell} c_\ell^{sat} (1 + K_{v\ell} V_v / V_\ell);$$

$$B \equiv K_{m\ell} (c_{surf} - cmc) + 1 + K_{v\ell} V_v / V_\ell + N K_{m\ell} c_\ell^{sat};$$

$$C \equiv N \text{ ; and}$$

$$N \equiv n_{tot} / (c_\ell^{sat} V_\ell) \quad (12)$$

In Figure 3a, solid curves for $n_{tot}/(c_\ell^{sat} V_\ell) = 18$ and 37 were generated using eqs 11 and 12, with values for the *cmc* and $K_{m\ell}$ (*cmc* = 8.27 mM, $K_{m\ell} = 1700\ M^{-1}$) taken from fits to the data at low limonene concentrations. These values in eq 9 yielded values of $c_{surf,o}$ of 16 and 24 mM, for $n_{tot}/(c_\ell^{sat} V_\ell) = 18$ and 37, respectively. Although there is reasonable agreement between theory and data in Figure 3a, it appears that these predictions for $c_{surf,o}$ are somewhat higher than those observed experimentally, and the theoretical curves are shifted to the right relative to the data. This discrepancy is removed by using a higher value of $K_{m\ell} = 2000\ M^{-1}$, as shown by the theoretical curves in Figure 3b. With this higher value for the micelle/water partition coefficient, both the break point $c_{surf,o}$ and the subsequent reduction in the vapor phase concentration are captured quantitatively. This good agreement suggests that the partition coefficient $K_{m\ell}$ may not be independent of limonene concentration, but may in fact be higher in micellar solutions with higher levels of limonene. This possibility will be addressed further in the next section.

Solubilization Isotherms: Distribution Behavior as a Function of Solute Concentration. A final set of experimental results is presented in Figure 4, representing HS-SPME measurements in vials containing various total concentrations of limonene, but at a fixed SDS concentration of 0.015 M. This surfactant concentration is almost twice the *cmc*, and thus micelles are present in all of these samples. On the basis of the discussion in the section above, we can see that the limonene concentrations used should fall into one of three regimes:

(I) low concentrations, $n_{tot}/(c_\ell^{sat} V_\ell) < (1 + K_{v\ell} V_v / V_\ell)$, such that all limonene would be soluble in the water phase even in the absence of micelles;

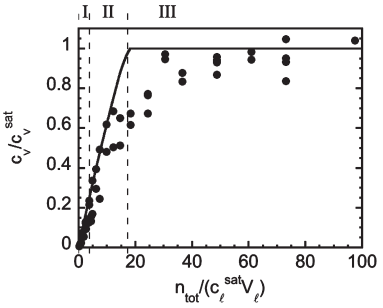

Figure 4. Normalized vapor phase concentration of limonene above a 0.015 M aqueous SDS solution, at various limonene levels ($n_{tot}/(c_\ell^{sat} V_\ell)$). Lines are predictions of eq 11 with $K_{m\ell} = 1700\ M^{-1}$. Low (I), intermediate (II), and high (III) concentration regions as defined in the text are indicated.

(II) intermediate concentrations, $(1 + K_{v\ell} V_v / V_\ell) < n_{tot}/(c_\ell^{sat} V_\ell) < (1 + K_{v\ell} V_v / V_\ell + K_{m\ell}(c_{surf} - cmc)/(1 - K_{m\ell} c_\ell^{sat}))$, which are above the solubility limit for water in the absence of micelles, but low enough that the limonene can be completely solubilized by the micelles; and

(III) high concentrations, $n_{tot}/(c_\ell^{sat} V_\ell) > (1 + K_{v\ell} V_v / V_\ell + K_{m\ell}(c_{surf} - cmc)/(1 - K_{m\ell} c_\ell^{sat}))$, such that the solute cannot be solubilized completely by the aqueous solution, and thus forms a bulk limonene phase.

Data in Figure 1 corresponded to the low concentration regime, whereas data in Figure 3 spanned intermediate and high concentrations. To relate our experiments to these different regimes, the total limonene amounts in the vial are plotted in Figure 4 as $n_{tot}/(c_\ell^{sat} V_\ell)$, using $c_\ell^{sat} = 1.01 \times 10^{-4}$ M.[33] The ordinate values in Figure 4 were obtained by normalizing measured peak areas above each sample vial by the peak area measured above a vial containing water and a separated limonene phase. The resulting ratio corresponds to c_v/c_v^{sat}. Assuming a constant value for $K_{m\ell}$, these data would obey eqs 11 and 12, so that, for low and intermediate concentrations, there would be an expected nearly linear relationship between c_v/c_v^{sat} and $n_{tot}/(c_\ell^{sat} V_\ell)$. This predicted curve should break at a value $n_{tot}/(c_\ell^{sat} V_\ell) \approx 1 + K_{v\ell} V_v / V_\ell + K_{m\ell}(c_{surf} - cmc)/(1 - K_{m\ell} c_\ell^{sat})$, where the limonene solubility in the micelle solution is exceeded. For higher values of $n_{tot}/(c_\ell^{sat} V_\ell)$, the vapor phase concentration would be predicted to remain constant at $c_v/c_v^{sat} = 1$. These predictions are shown with the solid lines in Figure 4.

However, the measured vapor phase concentrations shown in Figure 4 in the intermediate and high concentration regions fall below the values predicted by eq 11 with $K_{m\ell} = 1700\ M^{-1}$. Instead, the measured c_v increased nonlinearly with increasing n_{tot}, and did not attain the value of $c_v/c_v^{sat} = 1$ until the total limonene concentration reached $n_{tot}/(c_\ell^{sat} V_\ell) \approx 60$, a value well above that predicted by $1 + K_{v\ell} V_v / V_\ell + K_{m\ell}(c_{surf} - cmc)/(1 - K_{m\ell} c_\ell^{sat}) = 17$ with $K_{m\ell} = 1700\ M^{-1}$. Apparently, the SDS solution is able to take up more limonene than predicted from the constant partitioning behavior observed at low limonene concentrations. Instead, partitioning into the micelle increases with increasing limonene content in the system, suggesting that increased incorporation of the solute within SDS micelles alters their structure in such a way as to enhance their capacity for the oil. Such enhancements in solubilization with increasing solute concentration have been observed previously with benzene

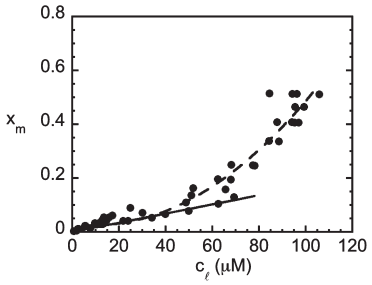

Figure 5. Mole fraction of limonene in micelles (x_m) as a function of the concentration c_{ℓ} of limonene dissolved in water. Solid line represents $x_m = K_{m/}c_{\ell}$ for $K_{m/} = 1700\ M^{-1}$. Dashed line is to guide the eye.

solutes in micelles.[28,47] This conclusion is also consistent with the results presented in Figure 3.

We can rearrange eq 1 to yield the mole fraction of limonene in the micelle x_m, given measured values for $c_v/c_v^{sat} = c_{\ell}/c_{\ell}^{sat}$ and known values for n_{tot}, n_{surf}, V_v, V_{ℓ}, $K_{v/}$, and c_{ℓ}^{sat}. The resulting isotherm of x_m versus c_{ℓ} is presented in Figure 5. At low c_{ℓ}, the mole fraction was proportional to aqueous limonene concentration as expected for a constant partition coefficient; the slope in this low concentration region is $K_{m/} = 1700\ M^{-1}$. As the aqueous limonene concentration increased, the solubilized mole fraction increased nonlinearly, corresponding to an increasing partition coefficient. At the upper end of the concentration range, the micelle consists of more than one-half limonene molecules, and its structure may be more properly characterized as an oil-in-water microemulsion droplet.

Tokuoka et al.[48] examined the ternary phase behavior of limonene−water−SDS mixtures at 30°C, and found an oil-in-water microemulsion region formed for SDS concentrations up to approximately 40 wt %. Maximum amounts of limonene per mole of surfactant were observed for SDS concentrations below 20 wt % and corresponded to limonene mole fractions of more than 0.5 within the micelles. At these high mole fractions, the energetic environment for a limonene molecule within the SDS/limonene aggregate is apparently more favorable than that in the SDS micelle that consists mainly of surfactant. The values indicated in Tokuoka et al.[48] correspond to a ratio $K_{m/} = x_m/c_{\ell}$ of approximately 5000 M^{-1}. The magnitude of this value is consistent with the reduction in c_v and nonlinear behavior that is observed in the Figure 4 data.

CONCLUSIONS

We have shown HS-SPME, combined with GC/MS, to be a convenient and effective method for quantifying the local distribution between micelles and water of the hydrophobic flavor compound limonene. At low total limonene concentrations in the liquid/vapor system, the distribution corresponds to a constant partition coefficient $K_{m/} = 1700\ M^{-1}$; the *cmc* can also be very accurately determined at these limonene concentrations. At higher limonene concentrations overall, the vapor phase concentration reflects the micellar solubilization capacity of the solution for limonene at a particular surfactant concentration. By fixing the surfactant concentration and varying limonene in the closed system, we observed an increase in the micelle/water partition coefficient, as limonene occupies larger fractions of the micelle and influences its energetics.

AUTHOR INFORMATION

Corresponding Author

*Phone: (530) 752-5447. E-mail: srdungan@ucdavis.edu.

Present Addresses

[||]Campbell Soup Company, Camden, New Jersey 08103, United States.

ACKNOWLEDGMENT

This project was funded by USDA CSREES Project #07-35603-17739 and the UC Davis Robert Mondavi Institute Center for Advanced Methods and Materials Processing (RMI-CAMMP).

REFERENCES

(1) Cukierman, E.; Khan, D. R. *Biochem. Pharmacol.* **2010**, *80* 762–770.
(2) Shi, Y.; Porter, W.; Merdan, T.; Li, L. C. *Expert Opin. Drug Delivery* **2009**, *6*, 1261–1282.
(3) Cameotra, S. S.; Makkar, R. S. *Pure Appl. Chem.* **2010**, *82* 97–116.
(4) Laha, S.; Tansel, B.; Ussawarujikulchai, A. *J. Environ. Manage.* **2009**, *90*, 95–100.
(5) Huang, Q. R.; Yu, H. L.; Ru, Q. M. *J. Food Sci.* **2010**, *75* R50–R57.
(6) Patist, A.; Kanicky, J. R.; Shukla, P. K.; Shah, D. O. *J. Colloid Interface Sci.* **2002**, *245*, 1–15.
(7) Qu, Q.; Tucker, E.; Christian, S. D. *J. Inclusion Phenom. Macrocyclic Chem.* **2003**, *45*, 83–89.
(8) Garcia-Rio, L.; Leis, J. R.; Mejuto, J. C.; Perez-Lorenzo, M. *Pure Appl. Chem.* **2007**, *79*, 1111–1123.
(9) Huie, C. W. *Electrophoresis* **2006**, *27*, 60–75.
(10) Khaledi, M. G. *J. Chromatogr., A* **1997**, *780*, 3–40.
(11) Borel, P. *Clin. Chem. Lab. Med.* **2003**, *41*, 979–994.
(12) Reis, P.; Watzke, H.; Leser, M.; Holmberg, K.; Miller, R. *Biophys. Chem.* **2010**, *147*, 93–103.
(13) Lee, S.; Gan, J.; Liu, W. P.; Anderson, M. A. *Environ. Sci. Technol.* **2003**, *37*, 5597–5602.
(14) Vaes, W. H. J.; Ramos, E. U.; Hamwijk, C.; van Holsteijn, I.; Blaauboer, B. J.; Seinen, W.; Verhaar, H. J. M.; Hermens, J. L. M. *Chem. Res. Toxicol.* **1997**, *10*, 1067–1072.
(15) Vaes, W. H. J.; Ramos, E. U.; Verhaar, H. J. M.; Seinen, W.; Hermens, J. L. M. *Anal. Chem.* **1996**, *68*, 4463–4467.
(16) Yang, Z. Y.; Maruya, K. A.; Greenstein, D.; Tsukada, D.; Zeng, E. Y. *Chemosphere* **2008**, *72*, 1435–1440.
(17) Auger, R. L.; Jacobson, A. M.; Domach, M. M. *Environ. Sci. Technol.* **1995**, *29*, 1273–1278.
(18) Micke, G. A.; Moraes, E. P.; Farah, J. P. S.; Tavares, M. F. M. *J. Chromatogr., A* **2003**, *1004*, 131–143.
(19) Delisi, R.; Genova, C.; Liveri, V. T. *J. Colloid Interface Sci.* **1983**, *95*, 428–434.
(20) Iwunze, M. O. *J. Mol. Liq.* **2004**, *111*, 161–165.
(21) Lissi, E.; Abuin, E.; Espinoza, C.; Rubio, M. A. *Langmuir* **1994**, *10*, 1071–1074.
(22) Nikiforova, E. M.; Bryleva, E. Y.; McHedlov-Petrosyan, N. O. *Russ. J. Phys. Chem. A* **2008**, *82*, 1434–1437.
(23) Sarma, S.; Bora, M.; Dutta, R. K. *Colloids Surf., A* **2005**, *256* 105–110.
(24) Sharma, N.; Jain, S. K.; Rastogi, R. C. *Spectrochim. Acta, Part A* **2007**, *68*, 927–941.
(25) Toki, T.; Shimeno, T.; Tominaga, T. *J. Chem. Eng. Data* **2010**, *55*, 2017–2020.
(26) Gadelle, F.; Koros, W. J.; Schechter, R. S. *J. Colloid Interface Sci.* **1995**, *170*, 57–64.

(27) Hussam, A.; Basu, S. C.; Hixon, M.; Olumee, Z. *Anal. Chem.* **1995**, *67*, 1459–1464.
(28) Liu, S. Y.; Davis, J. M. *J. Chromatogr., A* **2007**, *1147*, 111–119.
(29) Morgan, M. E.; Uchiyama, H.; Christian, S. D.; Tucker, E. E.; Scamehorn, J. F. *Langmuir* **1994**, *10*, 2170–2176.
(30) Vitha, M. F.; Dallas, A. J.; Carr, P. W. *J. Phys. Chem.* **1996**, *100*, 5050–5062.
(31) Hayase, K.; Hayano, S. *Bull. Chem. Soc. Jpn.* **1977**, *50*, 83–85.
(32) Quina, F. H.; Alonso, E. O.; Farah, J. P. S. *J. Phys. Chem.* **1995**, *99*, 11708–11714.
(33) Massaldi, H. A.; King, C. J. *J. Chem. Eng. Data* **1973**, *18* 393–397.
(34) Pino, V.; Ayala, J. H.; Gonzalez, V.; Afonso, A. M. *Anal. Chem.* **2004**, *76*, 4572–4578.
(35) Pino, V.; Afonso, A. M.; Ayala, J. H.; Gonzalez, V. *Anal. Bioanal. Chem.* **2007**, *387*, 2271–2281.
(36) Pino, V.; Conde, F. J.; Ayala, J. H.; Afonso, A. M.; Gonzalez, V. *J. Chromatogr., A* **2005**, *1099*, 64–74.
(37) Katsuta, S.; Saitoh, K. *Anal. Chem.* **1998**, *70*, 1389–1393.
(38) Lee, B. H.; Christian, S. D.; Tucker, E. E.; Scamehorn, J. F. *Langmuir* **1990**, *6*, 230–235.
(39) Choucair, A.; Eisenberg, A. *J. Am. Chem. Soc.* **2003**, *125*, 11993–12000.
(40) Rouse, J. D.; Sabatini, D. A.; Deeds, N. E.; Brown, R. E.; Harwell, J. H. *Environ. Sci. Technol.* **1995**, *29*, 2484–2489.
(41) van Os, N. M.; Haak, J. R.; Rupert, L. A. M. *Physico-Chemical Properties of Selected Anionic, Cationic and Nonionic Surfactants*; Elsevier: Amsterdam, 1993.
(42) Kardaras, E. *Partitioning Behavior of Limonene in a Sodium Dodecyl Sulfate Surfactant System*; University of California: Davis, CA, 2009.
(43) Lloyd, N. W.; Dungan, S. R.; Ebeler, S. E. *Analyst* **2011**, *136* 3375–3383.
(44) Lloyd, N. W. *Partitioning and Transport in Complex Nano-Structured Systems: Gradient Diffusion of Ionic Micelles in Gels and Partitioning of Hydrophobic Aroma Compounds*; University of California: Davis, CA, 2010.
(45) Helburn, R.; Albritton, J.; Howe, G.; Michael, L.; Franke, D. *J. Chem. Eng. Data* **2008**, *53*, 1071–1079.
(46) Hunter, R. J. *Foundations of Colloid Science*, 2nd ed.; Oxford University Press: Oxford, 2001.
(47) Tucker, E. E.; Christian, S. D. *Faraday Symp. Chem. Soc.* **1982**, 11–24.
(48) Tokuoka, Y.; Uchiyama, H.; Abe, M. *Colloid Polym. Sci.* **1994**, *272*, 317–323.